

## **Radar monitoring of seasonal bird migration over Central Israel**

L. Dinevich, Y. Leshem

*George S. Wise Faculty of Natural Sciences, Dept. of Zoology, Tel-Aviv University, Ramat Aviv, 69978, Israel.*

*E-mail: [dinevich@barak-online.net](mailto:dinevich@barak-online.net)*

### **Abstract**

A radar ornithological station has been created based on the meteorological radar MRL-5 and a specially designed algorithm. The system enables to plot radar charts within the radius of 60 km combining meteorological data with vectors of bird field flying at different heights and pass these charts online over to air traffic control operators. The data accumulated in the study made it possible to obtain certain characteristics of seasonal bird migration over Central Israel. The system and the results of the study have become an integral part of ensuring air safety for Israeli military aircraft.

**Key words:** radar ornithology, radar meteorology, radar echo, birds, bird migration, ornithology, air traffic safety.

### **Introduction.**

The number of collisions between aircraft and birds directly depends on flight velocities, flight intensity and the concentration of both aircraft and birds in the air (Leshem and Gauthreaux, 1996; Yakobi, 1974). These collisions lead to loss of human life, highly expensive equipment and death of birds (Bahat and Ovadia, 2005; Thorpe, 2005; Richardson and West, 2005).

The problem is especially acute for military aviation. Striving towards high speeds and high maneuverability within significant height range, as well as towards optimum ratio between the net load capacity and the dead weight make it difficult to protect military planes from partial destruction caused by its collision with birds. In Israel, during the period and within the air layers of intensive seasonal bird migration the number of bird can reach over 500 species per square kilometer of air (Bruderer, 1992). At the same time, a relatively small territory and Israel's special situation in the region requires extremely high concentration of military aircraft in the air.

In order to develop a concept of coexistence of birds and aircraft within the common air space, one needs, first and foremost, to get a detailed picture of how birds use the air space, namely, to obtain data on maximum bird concentration, diurnal bird activity, as well as dominant directions, speeds and heights of large and small bird flocks engaged in intercontinental migration. These data can be successfully obtained with the help of radars that enable not only

to establish bird presence in the air, but also to measure online the abovementioned characteristics of bird lights within the radius available within the radar's range of coverage. A computerized ornithological radar system of this type was created in Israel for bird monitoring and has been used both for research and operational purposes ( Dinevich et al, 2000; Dinevich et al, 2004; Dinevich and Leshem, 2007).

The aim of this paper is to give a brief description of the system and to present some results of the research into the parameters of seasonal bird migration over central Israel.

### **The principles underlying the computerized bird migration monitoring system based on MRL-5 meteorological radar**

#### ***Theoretical essentials of using radars for bird monitoring***

Schaefer (1966,1968) and Shestakov(1971) measured the dielectric properties and calculated the electromagnetic constants typical of different parts of a bird's body. According to the calculations, 83% of a bird's mass is tissues with high water content and the mean complex conductivity of  $52-17\cdot i$ ; 17% of a bird's mass is adipose tissues, bones etc. with the mean of  $3-1\cdot i$ . if we average over these values taking into account the percentage of different body parts, we will obtain the mean value of the dielectric constant to be  $44-15\cdot i$ . Hence radar echo from birds depend mostly on the reflection from the globe-shaped body (71%) and less on the muscular stem of a wing (11%), the head (6%) and the neck (5%). The plumage has the least contribution to the reflected wave (<2%) just as the reflection from wings and legs (2 and 3%, respectively). соответственно). The complex conductivity of cloud drops at the temperature of  $20^{\circ}\text{C}$  ranges between  $78,5-12,3\cdot i$  for  $\lambda=10$  cm and  $34,2-35,9\cdot i$  for  $\lambda=1,24$ cm (Stepanenko,1973). Thus the reflectance of a large bulk of a bird's body is close to that of cloud drop and is sufficient, therefore, for radar monitoring of birds just as a radar monitors clouds, meteorological radars being suitable for this purpose. .

A review by Eastwood (1967) compares capabilities of various pulse radars for bird monitoring. In a number of works (Shupijatcky, 1959; Atlas, 1964; Chernikov, 1979; Stepanenko, 1973; Houghton, 1964; Larkin, Evans et al, 2002; Buurma, 1999; Ganja et al, 1991; Gauthreaux et al, 1998; Gauthreaux and Belser, 2003; Bruderer and Joss, 1969; Zrnic and Ryzhkov, 1998) different echo properties are presented that make it possible to recognize bird echoes against the background of other echoes and evaluation is made regarding application of various wave widths and radar types for bird monitoring.

In Israel, a two-wave high-grade meteorological radar MRL-5 has been used for bird monitoring. The radar is mainly intended for measuring the structure as well as the dynamic and microphysical parameters of cloud formations. The radar enables to simultaneously scan the surrounding on two wavelengths (3.3 cm and 10 cm) using a narrow beam ( $0,5^{\circ}$  and  $1,5^{\circ}$ , respectively), the scanning being performed both by the azimuth ( $0-360^{\circ}$ ) and by the elevation within the upper hemisphere ( $-2 \div + 90^{\circ}$ ). The main parameters of the radar station are presented in (Abshayev et al., 1980).

Operating MRL-5 simultaneously on both wavelengths allows to reach equality of radar scan ranges and of both transmitter-receivers. Using this mode of operations, the echo ratio at the two wavelengths is determined entirely by the properties of the target.

The MRL-5 used in Israel for ornithological purposes is computerized and equipped with a supplementary device for measuring fluctuations of radar targets echoes and with an auxiliary polarization device (see Appendix).

The accuracy and the resolution of MRL-5 in bird monitoring, as well as the limitation of surveillance range due to the Earth's curvature are described in (Dinevich and Kaplan, 2000).

Briefly, these limitations are the following.

Within short distances, the main factor that determines the possibility of locating low-flying birds is the values by which the antenna elevation exceeds a certain critical value that is equal to  $r \cdot \theta/2$  ( $r$  is the distance from the radar to the target,  $\theta$  is the magnitude of the beam). At longer distances, the elevation can be decreased, but then the curvature of the Earth will have an impact. Both factors can be taken into account in the formula stating the dependency between the minimum height (in m) at which a target is detectable and the distance (m), being the root of the sum of squares

$$h_{\min} > \sqrt{(r\theta/2)^2 + 3,25 \times 10^{-15} r^4} \quad (1)$$

where the first item under the root depends on the beam width while the second one does not. As the width of the beam decreases, the radar's ability for detecting low-flying birds increases, however, the smallest extreme can not reach zero being dependent on the Earth's curvature. At regular refraction level, the radar being located at the sea level and the beam width of  $0,5^{\circ}$  (at 3.2 cm wavelength) the minimum height at which birds are detectable is: 100 m at the distance of 25 km; 350 m at the distance of 50 km and 1000 m at the distance of 100 km. If the radar is located above the sea level, these values decrease correspondingly. For example, the MRL-5 in Israel is located in Latrun at 270 m above the sea level. At the regular refraction level, at the distance of 25 km the radar detects all the birds flying at the level of the skyline ( $\theta = 0^{\circ}$ ) and

even at a certain negatively oriented angle. At the distances of 50 km and 100 km the radar detects birds flying at the heights of 100 m and 700 m, respectively.

In view of these considerations and based on the calculation of the Effective Scattering Area (ESA)  $\sigma_{cm^2}$  (see Appendix for more details on ESA) we see that at low heights the main factor that limits the distance of radar location of birds is not the station's potential but rather the Earth's curvature and the beam widths. According to experimental results, the ESA of a singly stork enables the MRL-5 in Latrun to locate it at the distance of 100 m if the bird is flying at the height not below 700m above the radar level.

**Selecting MRL-5 wavelength for bird monitoring.**

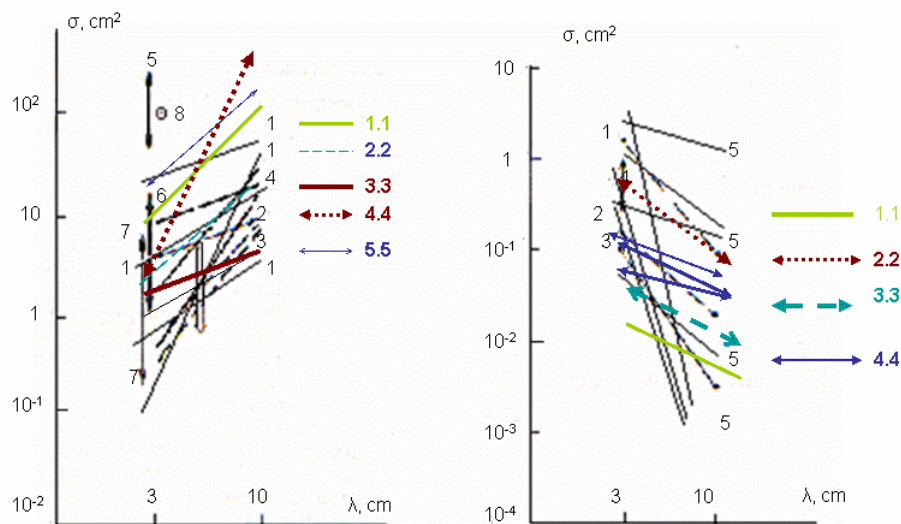


Fig. 1 Effective scattering area for birds and insects on two wavelengths (3cm and 10 cm).

a) 1.1; 2.2; 3.3; 5.5. – night-flying birds of various species ,4.4 - storks (Dinevich, MRL-5); 2. pigeons (Houghton); 3. sparrows (Konrad et ell.); 4. sea-gulls (Richardson et al.); 5. albatrosses (Rinehart ); 6. starlings (Houghton ); 7. sparrows (Houghton ).

b) 1. mantises (Glover et al); 2. bees (Chernikov); 3. dragonflies (Chernikov);  
1.1; 2.2; 3.3; 4.4 samples of night-time observations in Israel (Dinevich, MPJI-5).

Fig. 1 (a,b) presents birds' ESA measured at both radar wavelengths. For the sake of comparison, results obtained to this effect by other researches who used radars of different types are presented as well (Chernikov, 1979). We calculated the value of  $\sigma$  by the following formulas (Stepanenko, 1973):

$$\text{for } \lambda=3,2 \text{ cm, } \sigma_{\text{cm}}^2 = 0,6 \cdot 10^{-24} 10^{0,1n} R^4, \quad (2)$$

$$\text{for } \lambda=10 \text{ cm, } \sigma_{\text{cm}}^2 = 0,28 \cdot 10^{-25} 10^{0,1n} R^4. \quad (3)$$

where  $n$  is the radar reflectance of the target measured in dB and  $R$  is the distance to the target (m). The coefficients in the formulas are calculated based on values of the corresponding parameters of the antenna, the transmitters and the receivers. The principle used in the study for isolation of bird echoes is described in (Dinevich et al, 2001).

Fig. 1(a) shows that the bird ESA value on the second channel is greater than on the first one; our results are similar to findings those obtained by other authors (Chernikov, 1979). In some cases, authors attributed ESA with certain values to echoes from insects (Fig.1 (b)). Those ESA values are greater on 3-cm wavelength than on the 10-cm one. Visual observations made within the surface air (at nighttime) detected a significant increase in the number of insects (midges, moths, mosquitoes etc). The insects were clearly seen in the light of street lights, car lights and observed immediately at close distance. According to radiosonde data, higher humidity and light west-north/west breeze took place in the surface air at the time of these observations. For example, in case 2.2 presented in Fig. 1(b) (October 25, 21.30) the first inversion level was at the height of 800 – 1200 m; the moon was seen through ambient light. On both MRL-5 channels, a weak but spacious echo was detected, reflected from an invisible atmospheric formation about 500 m thick. One can assume the presence of vertical air flows in the bottom sub-inversion air layer, which led to buildup of different admixtures, among them insects. A characteristic feature of this echo was the difference between the values of differential reflectance measured at its top and bottom levels. Differential reflectance was measured by the dependency  $dP=P_{||}/P_{\perp}$ , where  $dP$  is the differential reflectance (a dimensionless quantity,  $P_{||}$  is the power of the reflected signal in mW (a wave of horizontal polarization was transmitted and received) and  $P_{\perp}$  is the power of the reflected signal in mW (a wave of vertical polarization was transmitted and received). The wave's polarization was altered pulse-by-pulse. At the rate of 500 pulse per second the frequency of polarization alteration is 1.500 sec. Within a time segment that short, positions of the targets relevant for our tasks (clouds, atmospheric inhomogeneities or birds) can not change.

The value of differential reflectance in the top part of the echo was close to unity (or 0 dB) which is typical of reflections either from globular cloud particles or the boundaries of

atmospheric layers with a high temperature-humidity gradient (Chernikov, Shupiatsky, 1967; Dinevich et al, 1990; Zrnic, Ryzhkov,1998).

This phenomenon can be accounted for by the isotropic reflection properties of atmospheric inhomogeneities (invisible thermics or mesofronts), small global cloud drops or small crystals with chaotic spatial orientation (though there could be no crystals in the case above considered). Differential reflectance of the lower part of the echo was  $>1$  which is typical of non-spherical reflectors horizontally oriented UN the space. (Dinevich et al, 1990, 1994). It suggests that the lower part of the echo was formed not only due to the temperature-humidity gradient, but also due to the horizontally-oriented doublets that are present in the sub-inversion level and that can be caused only by insects or oblong plant seeds. In addition, it should be noted that, according to the radiosonde readings that were closest in time, all these echoes shifted under the direction of and at the velocity of wind at the height. Thus, one can conclude that the echoes we observed within the sub-inversion level on both radar channels were echoes from insects. In all the cases, the ESA on th3 3-cm wavelength was greater than that on the 10-cb band, which well agrees with findings by other authors (Glover, Hardy, 1966; Chernikov, 1979).

The results of the observations showed that the 10-cm band is more efficient for bird monitoring, i.e. both the number of birds located and the distance of location are higher. This can be attributed to the higher potential of the band and a wider beam that is able to cover birds from a lager space, as well as to the general laws of dispersion for different ratios of a target dimensions and the wave lengths.

In view of all these considerations, the second channel, namely, the 10-cm band was chosen for bird monitoring ( $\lambda=10\text{cm}$ ).

Taking into account the diversity of radar targets in the atmosphere (clouds, precipitation, invisible atmospheric inhomogeneities, aircraft etc.), the nail goal of the study is finding the properties that are typical of bird radar echo.

***Table 1. Reflectors typically present within bird monitoring area***

Table 1 presents the most typical reflectors and their echo properties.

\* only a few of the scholars who studies echo properties from various reflectors are mentioned in the table.

Reflectors	Characteristic echo properties	Reserachers*
Ground clutter (hills, buildings, trees).	Occupy large space, high power, wide fluctuation spectrum both by amplitude and by frequency, relative immobility	Atlas, 1967; Hajovsky et al, 1966; Chernikov, 1979
Clouds of different types, including convective and stratus clouds.	Occupy large space, shift along the direction of the dominant wind flow. Unlike bird echo, the echo from atomized clouds and precipitation is larger at 3cm wavelength than on 10cm one. Echo from globular clouds, at both	Atlas, 1967; Shupijatcky, 1959; Chernikov, 1979; Stepanenko, 1973; Doviak, Zrnic, 1984;

	wavelengths, are significantly larger than bird echo. Polarization parameters of signals in atomized clouds are typical of spherical targets. Differential reflectivity, being the ratio between horizontally oriented reflected signal (when the radiated signal is horizontally polarized) to vertically oriented signal (when the radiated signal is vertically polarized) Is close to unity for small drops. Although clouds evolve in time and space, echo from them remains for a long time located in the same coordinate points, unlike echo from birds.	Dinevich et al, 1990, 1994; Zrnic and Ry Ryzhkov, 1998.
Invisible atmospheric inhomogeneties	Low power, chaotic shift patterns in space. Polarization echo parameters are close to similar parameters of spherical hydrometeors.	Shupijatcky, 1959; Battan, 1963b; Lofgren, Battan, 1969; Khardy, 1969; Kropfli, 1970; Chernikov, 1979; Сальман, Брылёв, 1961; Doviak, Zrnic, 1984; Zrnic and Ryzhkov, 1998; Venema, Russchenberg et al, 2000.
Aircraft	Significant powers. High shift velocities.	Daniel et al, 1999; Skolnik, 1970.
Active noise caused by outside radiators (nearby radars)	Radial orientation, random pattern of signals in time and space.	Skolnik., 1970; Dinevich et al, 2001.
Insects	Low power, the direction and velocity of shift coincide with wind direction. ESA at 3 cm wavelength is larger than that on 10 cm wavelength.	Hajovsky et al, 1966; Glover, Hardy, 1966; Skolnik, 1970.
Birds	Relatively low power $O Z < 30 \text{ dBZ}$ , forward and relatively straightforward movement, maximum amplitude fluctuations within the low-frequency range (up to 10dB within the frequency range of 2-50Hz). Echo is larger on 10 cm wavelength than on 3 cm one. Polarization parameters of signal are characteristic of horizontally oriented targets. Differential reflectivity is significantly higher than unity. The mean ESA** values of different bird species at the value of radar wavelength less than 10 cm or $15 \text{ cm}^2$ (Sparrow) до $400 \text{ cm}^2$ (Albatross).	

Table 2 presents ESA ( $\sigma$ ) for different bird species at the wavelength  $\lambda = 10 \text{ cm}$ .

**Table 2.  $\sigma$  values for different bird species with wings folded measured at different body positions orientation relative to the radar (data obtained by Zavirukha, Stepanenko, 1978)**

Bird species	$\sigma \text{ m}^2$ value of birds exposed to radiation in different projections		
	Side	Head	Tail
Rook	$2.5 \cdot 10^{-2}$	-	-
Pigeon	$1.0 \cdot 10^{-2}$	$1.1 \cdot 10^{-4}$	$1.0 \cdot 10^{-4}$
Starling	$2.5 \cdot 10^{-3}$	$1.8 \cdot 10^{-4}$	$1.3 \cdot 10^{-4}$
Domestic sparrow	$7.0 \cdot 10^{-4}$	$2.5 \cdot 10^{-5}$	$1.8 \cdot 10^{-5}$

The ESA value of the same bird can alter by factor of 10 depending on the bird's body position relative to a radar (Houghton, 1964, Eastwood, 1967, Bruderer and Joss, 1969). The data obtained in bird ESA measurements in an anechoic room at different angles relative to the radar beam (Zavirukha, Stepanenko, 1978) found the echo maximum to be between 65 and 115 degrees relative to the radiation beam, which corresponds to the side-ward exposure (beam directed onto a bird's beak is assumed to be  $0^0$ ). Besides, variations in ESA values can be caused by wing flapping, when the value can increase by factor of 10 or drop down to almost zero. The frequency of these fluctuations can reach 2-24 Hz (Chernikov, 1979). Therefore, ESA of a bird depends on its dimensions, its body projection relative to the radar and the instant configuration of the flapping wings. Hence alterations in the amplitude of an echo reflected from a single bird flying at the same body angle relative to the radar will depend entirely on the wing flapping frequency. The research we conducted into fluctuation characteristics of different types of reflectors enabled to find a fluctuation pattern specific only for birds. On the basis of this pattern and a vast statistics obtained concerning different types of reflectors, a special low-frequency filter was developed for isolating bird echoes (Dinevich et al, 2004). The filter enables, at radar antenna halted, to isolate averaged 1-15-sec echo samples reflected from a bird flock at the accuracy of over 80%, and echoes from a single bird at the accuracy up to 95%. Several researchers (Shupijatsky, 1959; Houghton, 1964; Chernikov, Schupjatsky, 1967; Lofgren, Battan, 1969) point to a distinct dependence of bird ESA on the polarization of the signal both transmitted and received, as well as on bird's body position relative to the radar. According to (Chernikov, Schupjatsky, 1967), the depolarization degree for bird echoes is about dB. For a polarimeter with a linear depolarization of transmission and reception, depolarization is defined as the ratio between the values of the main component of the reflected signal and its orthogonal component. In case the waves have horizontal polarization, the depolarization expression can be written as

$$\Delta P_x = P_{xy}/P_{xx} \text{ or } \Delta P_x \text{ (дБ)} = 10 \lg P_{xy}/P_{xx} \quad (4)$$

In case of vertical wave polarization, the expression is written as  $\Delta P_y = P_{yx}/P_{yy}$ . Here,  $P_{xx}$ ,  $P_{yy}$ ,  $P_{xy}$ ,  $P_{yx}$  stand for the components of the received signal power, where the first index is the transmittance polarization type and the second index is the reception polarization type, while x and y stand for the horizontal and vertical polarization, respectively.

In case of pulse-by-pulse alteration of polarization while transmitting and receiving the same signals, differential polarization can be calculated as

$$dP = P_{xx}/P_{yy} \text{ or } dP = 10 \lg P_{xx}/P_{yy} \quad (5)$$

In a number of studies (Shupijatcky, 1959; Dinevich, Kapitalchuk, Schupjatsky, 1990, 1994) it was shown that values of depolarization and of differential polarization are functionally related only to the shape of the target and its orientation in space, while being independent from other parameters including the permittivity, signal attenuation etc. Using the two polarization components  $\Delta P_x$  and  $dP$ , one can calculate birds' orientation in space and their shape, i.e. the ration between the length and the width.

The formula for calculating the angle of a bird's spatial orientation (Shupijatcky, 1959) is  $\text{tg}2\theta = 2 dP^{1/2} \Delta P^{1/2} [dP^{1/2} - 1]$  (6),

where  $\theta$  is the angle of a bird's spatial orientation. The opportunity of isolating bird echo by polarization properties is also mentioned by (Zrnic and Ryzhkov, 1998). It should be noted that identifying bird echo, either by polarization properties or fluctuation pattern, requires that a sufficient number of echoes is obtained enabling their averaging. According to experimental data, at the rate of 500 pulses per second it takes not less than 10 sec to obtain the requires number of echoes on the basis of the fluctuation pattern, and not less than half a second at each azimuth on the basis of polarization properties. This fact makes it difficult to use those properties for identifying echoes from large numbers of reflectors in real time within the radar scan range (e.g., 60 km in radius) with a rapidly rotating antenna.

As we see both from Tables 1 and 2, as well as from the above considerations, signals from all the reflectors mentioned not only have distinct features typical of a certain type of reflectors, but also vary within a wide dynamic changeability range. Due to this fact, all the properties described above, including fluctuation and polarization properties, can not be sufficient for online monitoring of the ornithological situation within radar scan range. It was necessary to find more distinctive properties that characterize bird radar echo.

These newly determined properties, as well as the algorithm of their application and the principles of the radar ornithological system based on MRL-5 radar are fully described in (Dinevich, Leshem, 2007). Here we will present the main principles of the solution and some examples of its practical implementation in monitoring bird migration.

### **The Algorithm Scheme**

Digitalized signals are entered into the computer and undergo limitation and filtration procedures. In order to increase the "signal/noise" ratio signals obtained over several pulses are summated (usually 16 pulses). Periodically, signals undergo calibration using the design values of the radar constant and the receivers noise level.

For greater efficiency, data are collected more often than it is required due to the radar resolution by distance (Abshaev, Kaplan, Kapitannikov, 1984). Each bird is presented in the

coordinates “distance-angle” in the form of a spot rather than a dot. Resolution parameters of the radar and the registration system are shown in Table 3.

Таблица 3

	Radar	Registration
Resolution by azimuth	0.5 <sup>0</sup>	0.176 <sup>0</sup>
Resolution by distance	150 m	60 m

In the study described here we obtained a number of additional properties characteristics of a bird’s echo. They are related to the time and space patterns of birds’ behavior in the course of flying (Fig.2).

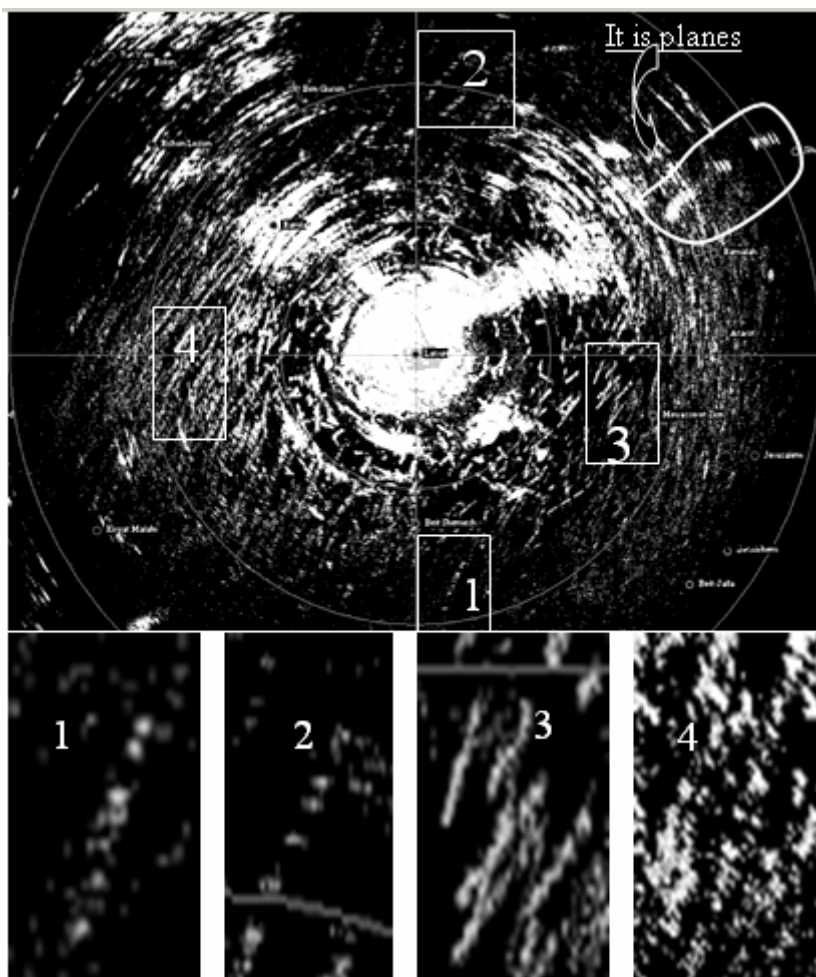


Fig.2. The echo field after digital processing. Lines formed by sequential dot-like echoes represent bird flight routes. Areal shapeless echoes are reflections from hills. The isolated fragments clearly show how bird flight route lines are being formed by dot-like bird echoes, among them:

1. a single bird of a single bird group,
2. two birds or two bird groups,
3. several birds or several bird groups.,
4. many birds or many bird groups within a zone of high bird density.

Fig.2 shows the total echo field over 18 scans after digital processing. On can clearly see the dot structure of echo streaks obtained from flying birds. Thus, an essential property of bird echo is the character of its motion resulting in transformation of a set of dots into streaks. As can be

seen from the enlarged fragments (1,2,3,4) the streaks are relatively straightforward. The increment in the streak length is due to the straightforward motion of echo in time.

It is noteworthy that, at the same coordinate point, echoes from ground clutter, clouds and other spacious targets remain unchanged from scan to scan. Only bird echoes change, being characterized by small dimensions and mobility. In we remove all echoes that at the same coordinate point remain unchanged more than a set number of times (1-2) from a summated echo obtained over several scans, we can say with high certainty that signals remaining are entirely bird echoes. In order to analyze echoes obtained within a hemisphere, the radar must scan the space within a preset range several times, each time at a different tilt. The duration of a single scan is 10 sec, the number of scans at the same tilt was experimentally determined to be 8, and the number of tilts, usually not exceeding 6, depends on the beam dimensions and bird flight heights. Further analysis of signals thus selected enables to perform an additional filtration of bird echoes and to plot corresponding vectors representing their flight direction, velocity and height.

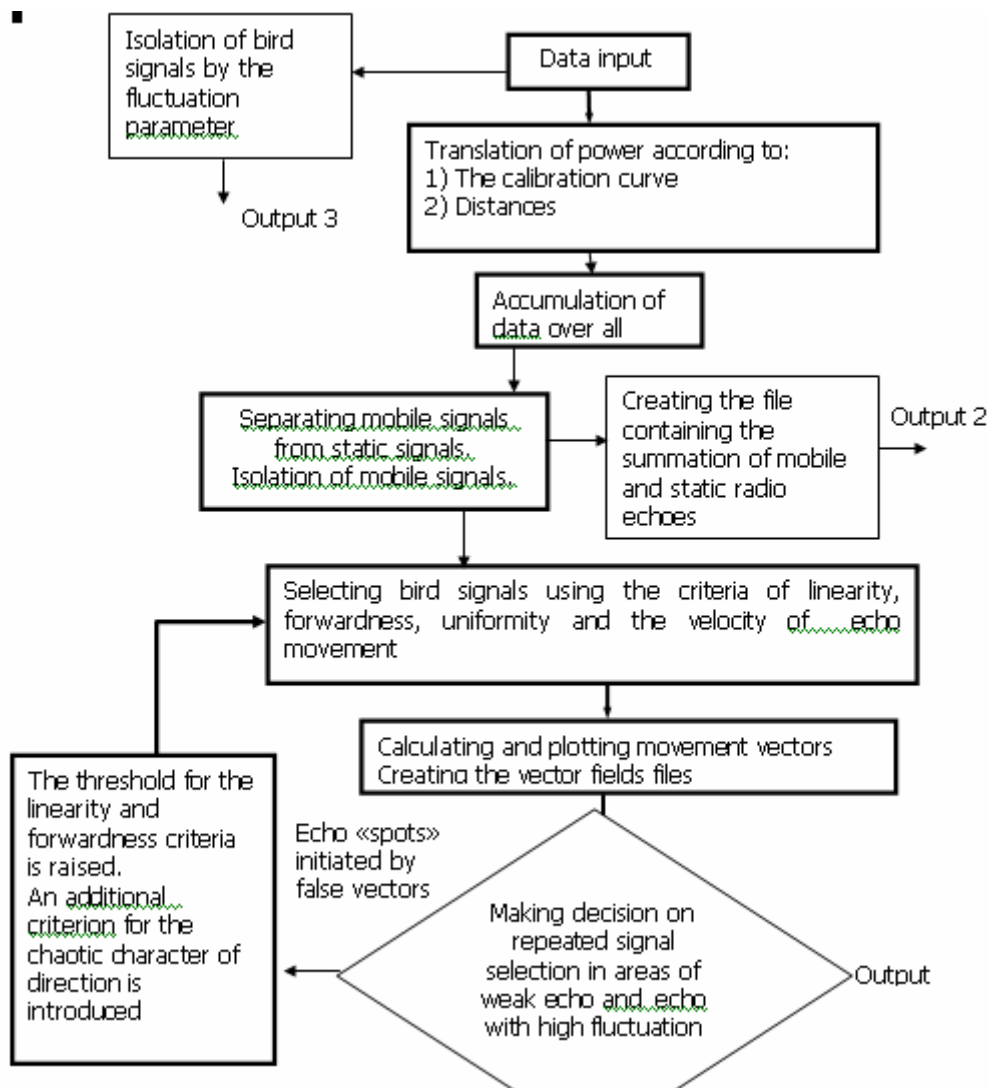


Fig.. 3 Flow chart of the algorithm for identifying birds and measuring their flight velocities.

Fig.3 shows the flow chart of the algorithm used for bird identification and measuring their flight velocities. The algorithm includes several stages of echo field processing, the main stages being:

- analyzing echo power;
- excluding echoes whose power is below the noise level and above theoretical maximum of a bird echo;
- summation of all remaining echoes over a preset number of scans (in this study, 8 scans were chosen as a result of experiments)
- isolation of a single bird (bird group) from other reflectors by selecting bird echoes on the basis of motion and the motion pattern;
- calculating velocity vector for each bird (bird group);
- excluding false vectors using a special method of analyzing vector fields based on additional properties (values of radar reflectance, velocities and the degree of chaotic state in flight directions);
- plotting ornithological charts of several kinds.

For each bird echo thus isolated, the location of the echo's center of gravity is calculated taking into account the echo's power

$$\bar{X}(j) = \sum_i S_{ij} X_i / \sum_i S_{ij} \quad \bar{Y}(j) = \sum_i S_{ij} Y_i / \sum_i S_{ij} \quad (7)$$

where  $S_{ij}$  is a signal power value,  $i$  is the number of a point within each scan and  $j$  is the number of a scan.

On the basis of values  $\bar{X}(j)$ ,  $\bar{Y}(j)$ ,  $t(j)$  (time) root-mean-square linear regression dependencies  $X(t)$ ,  $Y(t)$ ,  $Y(X)$  are formulated. Tangents of angles of slope for dependencies  $X(t)$  and  $Y(t)$  serve as evaluations of bird's velocity components  $V_x$  and  $V_y$ . Correlation coefficients  $R_{xt}$ ,  $R_{yt}$ ,  $R_{xy}$  obtained as a result of forming said regression dependencies are modulus of precision in evaluating velocity components.

Performing all the stages of selection of reflected signals on the basis of properties described above (Dinevich, Leshem, 2007) we get a corpus of data obtained over a preset scan range, including separate data on echoes from different targets, such as ground clutter, clouds, precipitation, local and migrating birds etc.

**Graphic representation of bird monitoring data (including the background of hills and atmospheric formations)**

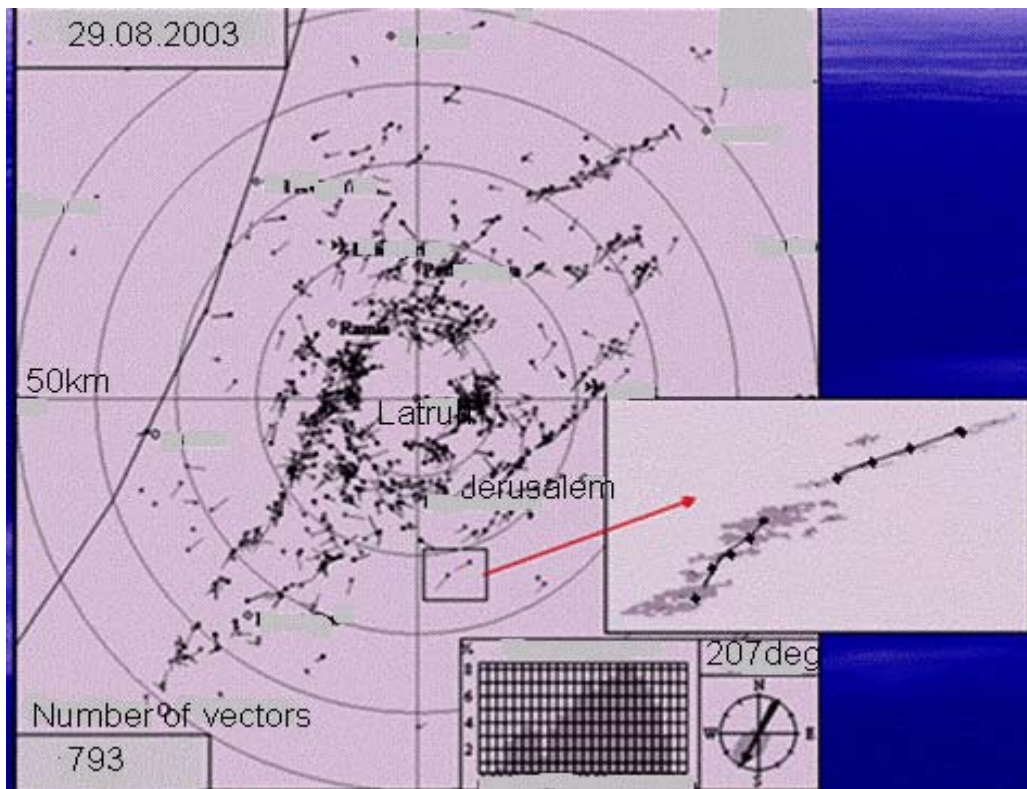


Fig. 4 Ornithological chart for 29.08.2003. Top part – direction towards the north. Thin solid line in the west – the border between the land and the sea. Streaks formed by vectors represent birds. An enlarged fragment showing two vectors enables to understand the principle of plotting two vectors formed by the centers of echoes gradually shifting from scan to scan.

Fig.4 presents a chart of bird vectors within the radar scan range. As an example, two vectors are shown enlarged together with the interim echo spots used for plotting these vectors.

The presence and the pattern of motion are the main characteristics underlying isolation of bird echoes against the background of other reflectors. The actual application of the selection procedure is described in detail in (Dinevich, Leshem, 2007). After we project bird echoes extracted from the summated data file onto a horizontal plane, we obtain vectors representing the birds within the radar scan range. If we map on this horizontal projection cursors, roads, cities, the coastline etc and orient the map along the cardinal directions, we will obtain a radar ornithological chart (analogous to a weather chart). The summated data file contains, besides the bird monitoring data, also some data on ground clutter, clouds, precipitation etc. Using colors or other symbols, we can present this information in ornithological charts.

By way of example, Fig. 5 (a) presents an ornithological chart (in 1:30 km scale) plotted for 21.10.2002, 8.20 a.m. For comparison, Fig. 5 (b) presents the total echo chart with bird echoes not isolated, and Fig. 5(c) shows the bird vector field against the background of ground clutter

( green-colored echo) and clouds (blue-colored echo).

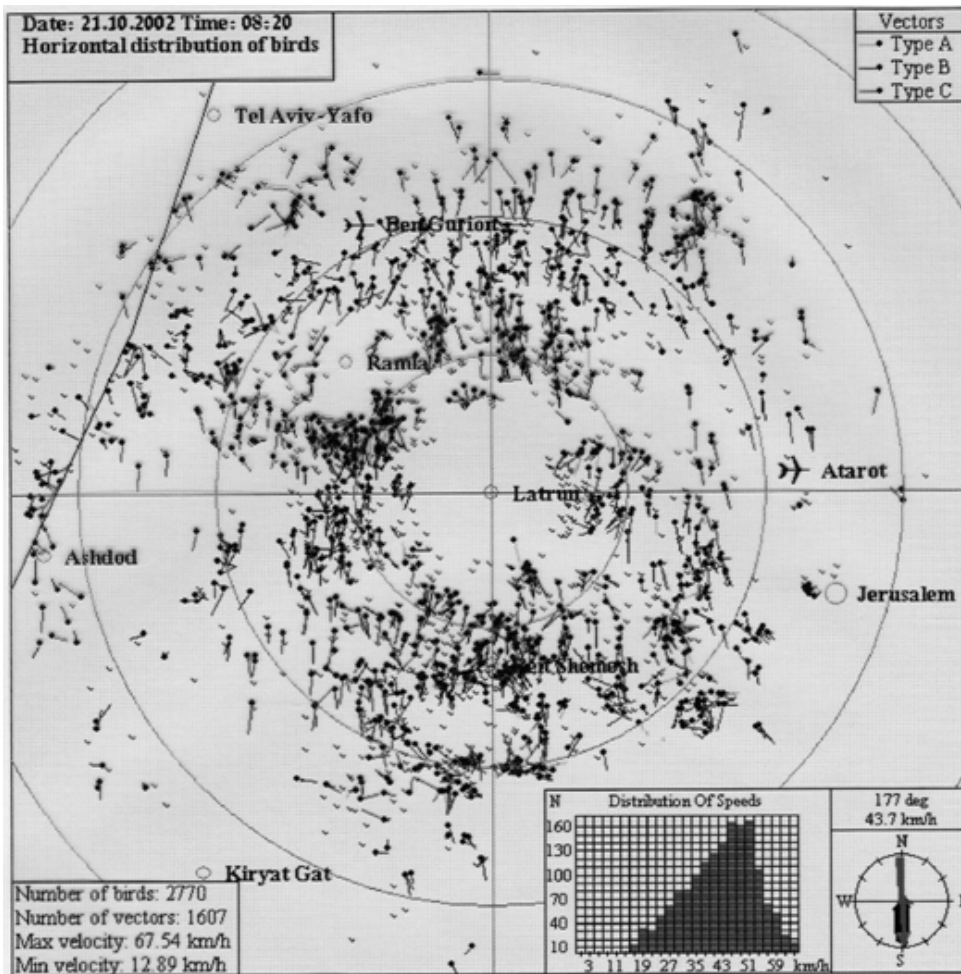


Fig. 5 (a). Ornithological chart in a vector form. Early morning.

∇ – local birds flying in sporadically changing directions; red vectors- birds, flying with unchanged direction and velocity for significant segments of time; blue vectors- birds flying in the same direction for significant segment of time but changing velocities; brown vectors – birds frequently changing both flight directions and velocities.

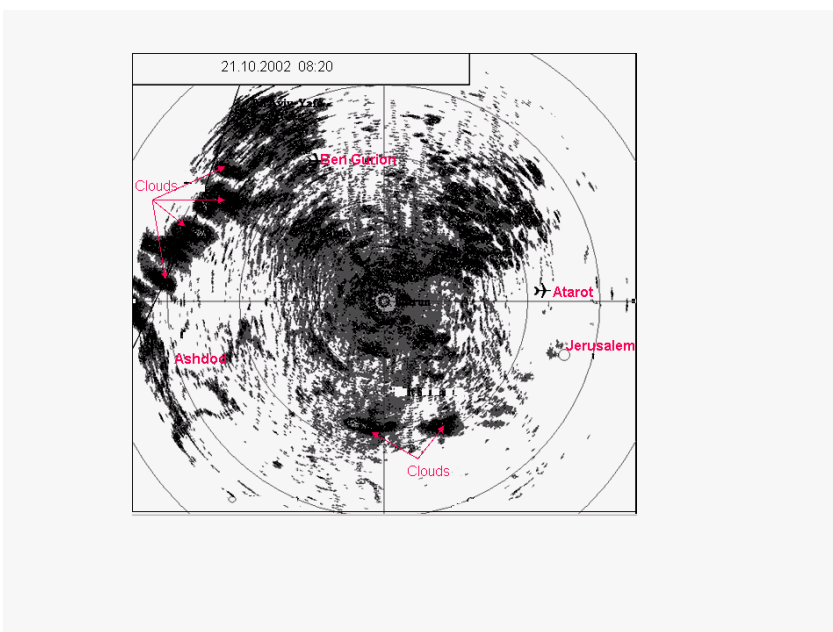


Рис. 5 (b) Chart of the total echo (Chart 4(a) before the algorithmic echo processing).

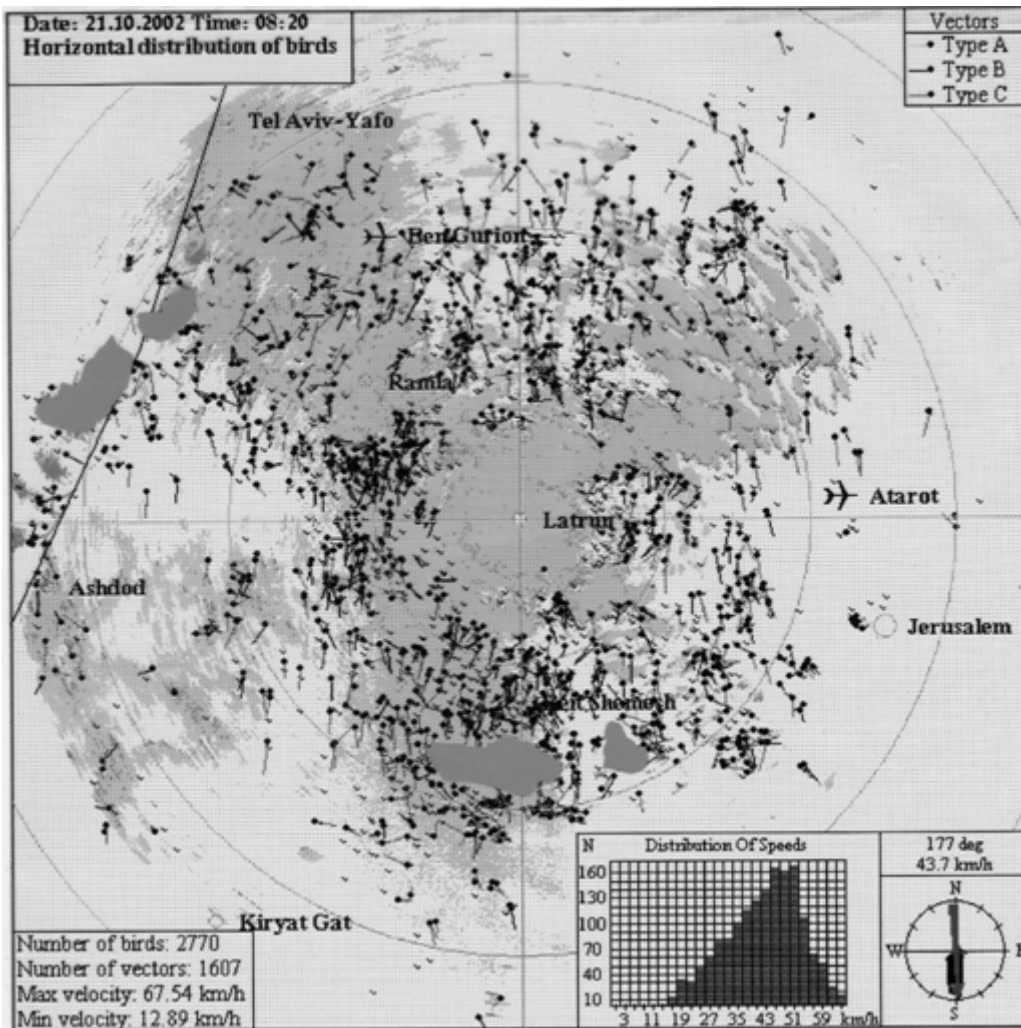


Fig. 5 (c) Ornithological hart against the background of ground clutter and atmospheric formations (ground clutter – green color, blue colored echo- clouds).

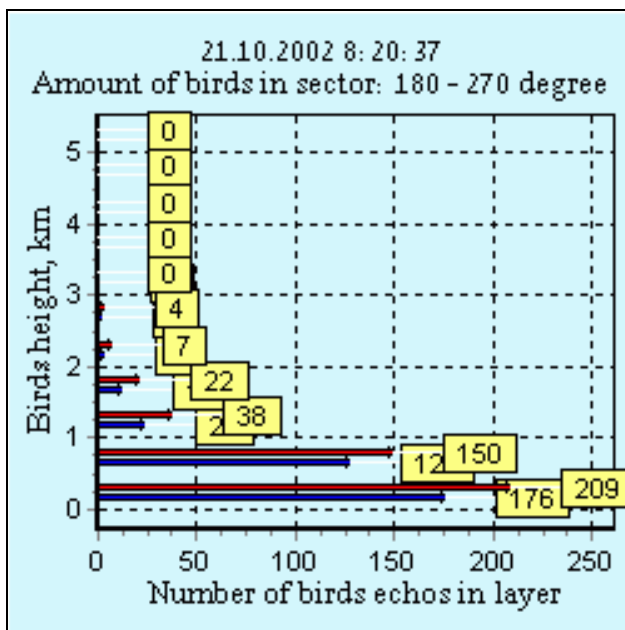


fig.5(d)) the maximum concentration of birds is observed within the layer up to 500 m from the ground surface (209 bird groups); a significant number of birds are flying within the 500-1000-

m layer (150 bird groups), while a small number of birds are found even in the layer of 1000-3000 m (13 bird groups were observed within 2000-3000-m layer).

Using the chart as an example, we may see the type and volume of information it contains:

1. The total number of birds within the 30-km distance range from the radar is 2770 (usually charts of this type are plotted in scales of 1:30, 1:40 and 1:60).

2. The number of echoes from birds flying in a certain direction (number of vectors) is 1670.

Different colors mark birds with different flight patterns: red – straightforward uniform motion; blue- straightforward non-uniform motion; brown- non-straightforward and non-uniform motion.

3. Maximum bird echo movement velocity relative to the radar is about 68 kmh.

4. Minimum bird echo shift velocity relative to the radar is about 13 kmh.

5. Most bird echoes move at the speed of 45-50 kmh.

6. The dominant flight direction is  $177^{\circ}$

7. The majority of birds fly at a variable speed and deviate from a linear direction; however, there are many birds that, while deviating from a linear direction, fly at a uniform speed.

8. Within the scan range against the ground clutter (hills), one can isolate several groups that differ in bird density.

9. Within the cloud layer, birds tend to fly around clouds over their perimeter or to squeeze through separate cloud cells (to the south of the radar, a bird flock is trying to fly between cloud cells 1 and 2).

10. Within the  $180^{\circ} - 270^{\circ}$  sector (see fig.5(d)) the maximum concentration of birds is observed within the layer up to 500 m from the ground surface (209 bird groups); a significant number of birds are flying within the 500-1000-m layer (150 bird groups), while a small number of birds are found even in the layer of 1000-3000 m (13 bird groups were observed within 2000-3000-m layer). A complete analysis of the ornithological situation enables to get all this information for the entire hemisphere ( $360^{\circ}$  sector). The red stripe shows the total number of birds within a layer (both local species flying about chaotically directions and migrating birds flying along a certain directions) while the blue stripe represents only migrating birds whose echoes can be used for plotting vectors.

The system enables to obtain this total data corpus within the radius of 60 km from the radar every 10-15 minutes online and to forward this information to any user via the Internet. In addition, there are several issues to mention:

Atmospheric formations out into in the charts described above enable only to get some data about their locations and shifts. More detailed information about atmospheric formations (clouds, precipitation, atmospheric inhomogeneities) can be found in other radar meteorological

charts that are plotted simultaneously with the ornithological ones but are based on data collected through different procedures. For example, one of the requirements for collecting such data is antenna elevation up to 85<sup>0</sup>). A sample of a meteorological chart is presented in (Dinevich et al, 2000).

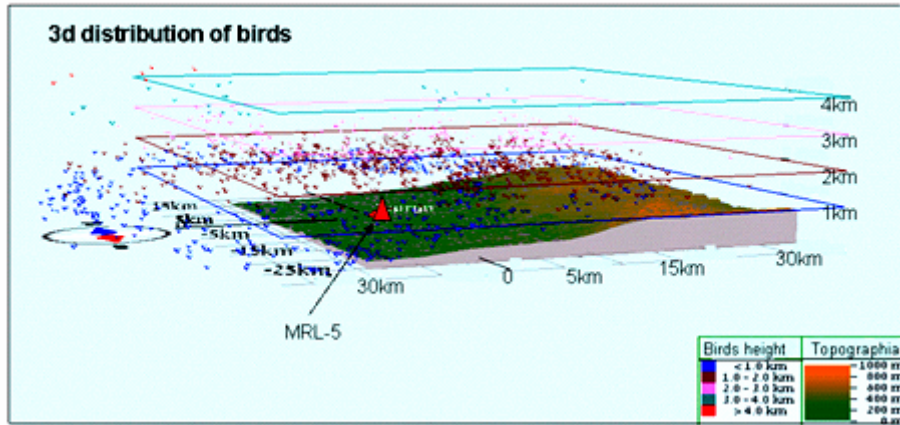


Fig. 6. A fragment of Fig. 4. Distribution of birds over vertical layers within a prescribed sector.

Fig.6 shows a sample of a volumetric picture of birds' distribution over a certain ground area. The arrow placed outside the figure points at the north. A symbol on the grounds stands for the radar location. In the west the terrain adjoins the costal line, in the east there are hills. Horizontal terrains lie at different heights. The software program enables to view this volumetric picture angle.

Each part of Fig. 7 (1, 1a – 11, 11a, 12) presents two samples of two types of charts illustrating changes in flight intensity for flocks of storks during day hours 29.08.2003.

In the left part of each chart one can see how echoes from airborne targets changed with time (hills, planes, atmospheric inhomogeneities, birds), while the right part presents the corresponding changes in vectors representing bird flights.

These examples are typical of two types of bird migration, namely, night flights including small hours of the morning when there are no ascending air flows (Fig.5) and daytime flights when there are convective flows in the troposphere (Fig.7). In the first case, the birds fly in large flocks over occupying large squares and within multiple heights. In the second case the bird flocks form long streaks (Leshem, Yom-Tov, 1998, 1996; Alpert, Tannhauser, 2000).

Experimental data obtained with the help of the developed algorithm enables to collect statistics statistic to evaluate some parameters of inter-seasonal bird migration over Central Israel.

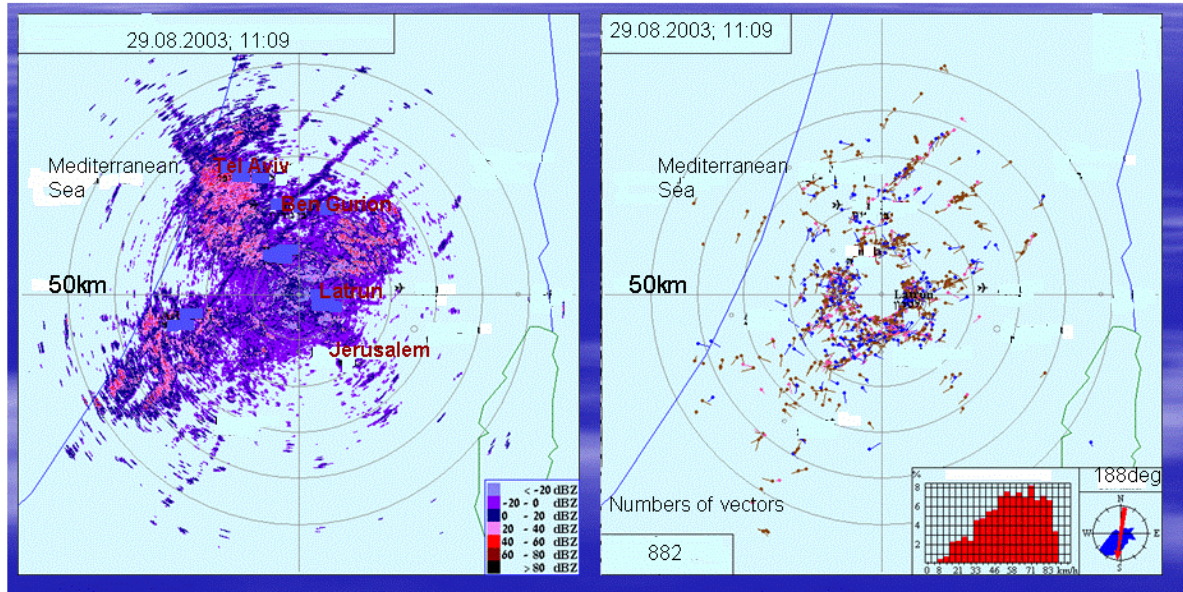


Fig.7 (1, 1a)

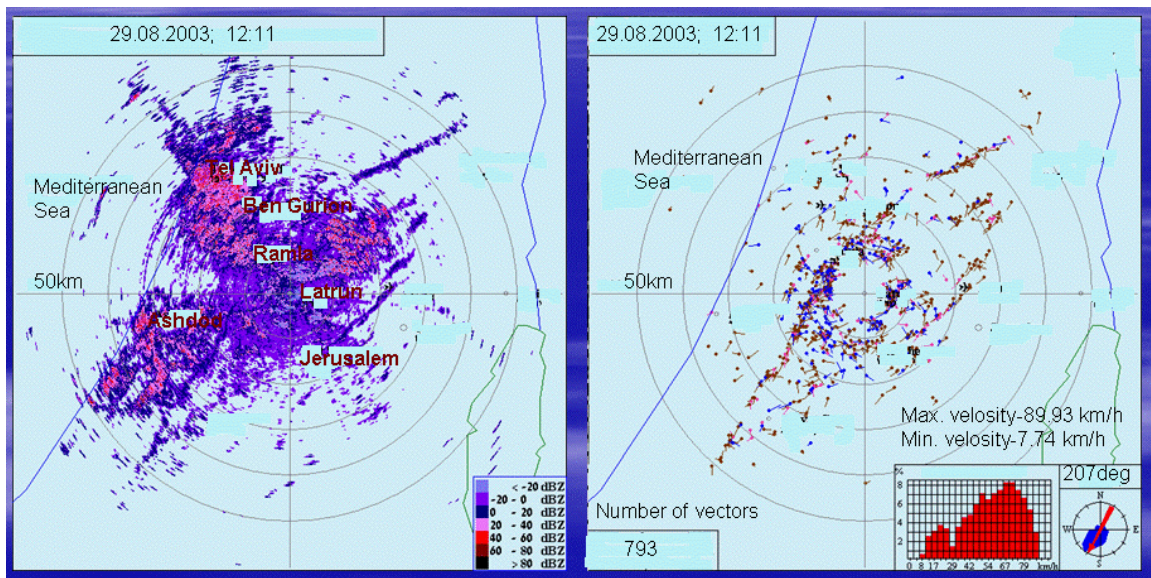


Fig.7 (2, 2a)

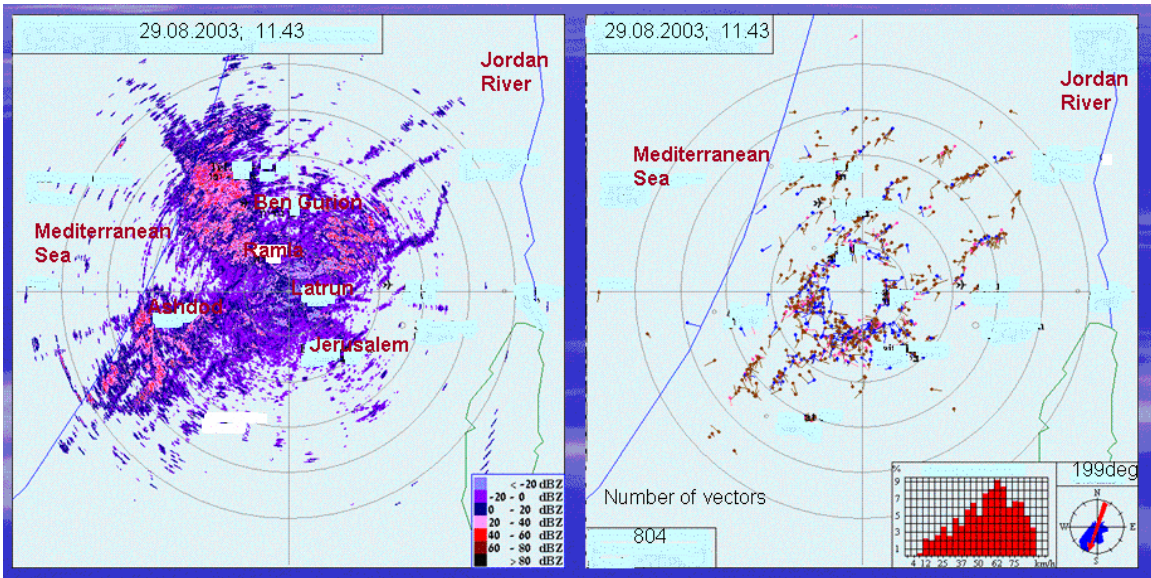


Fig. 7 (3, 3a)

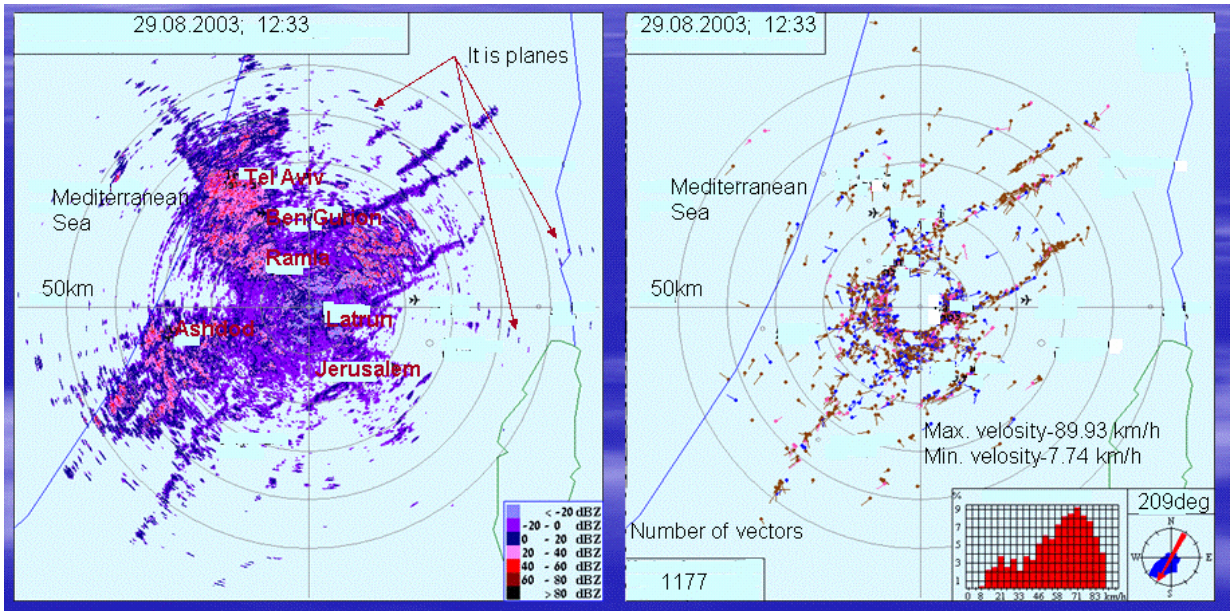


Fig. 7 (4, 4a)

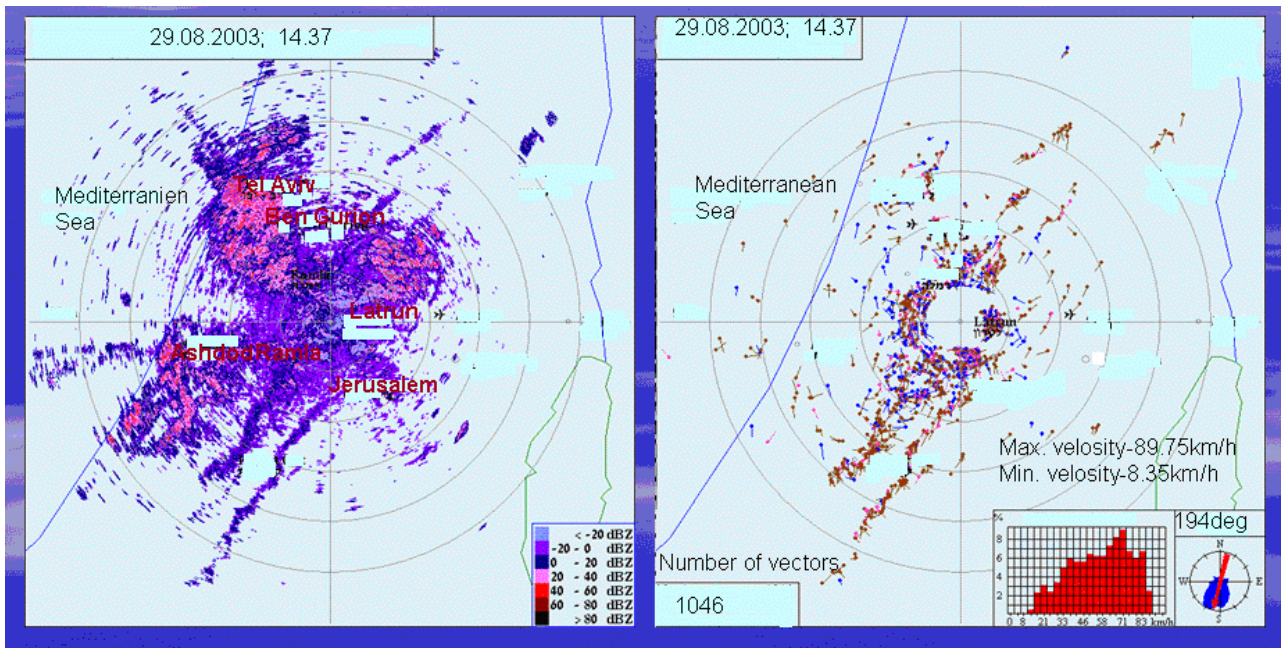


Fig.7 (5, 5a)

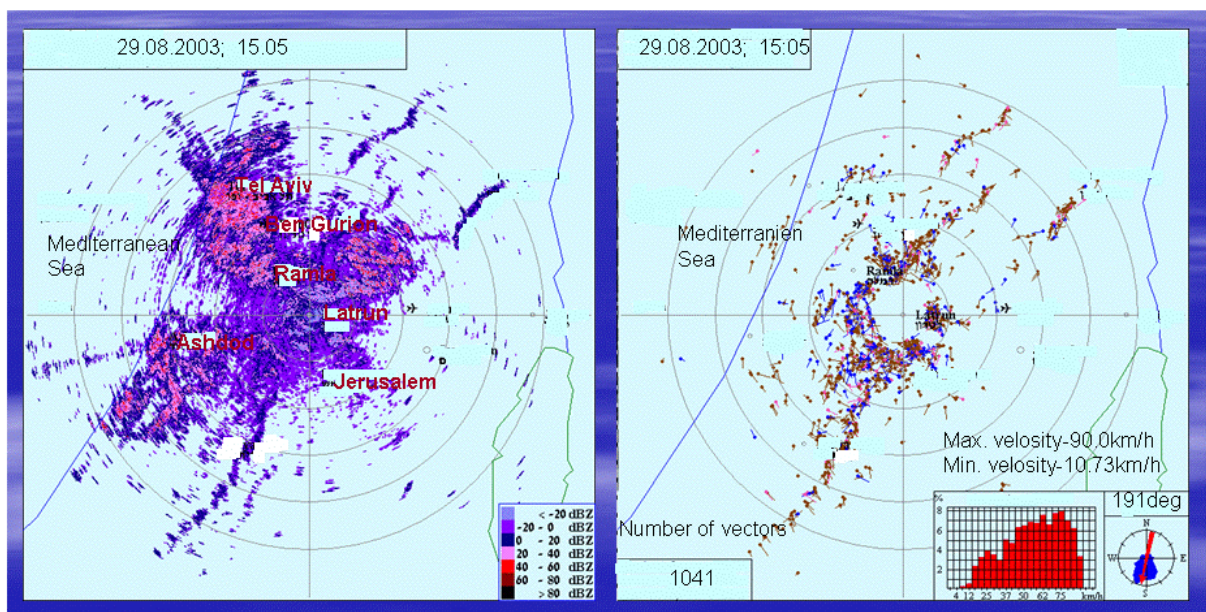


Fig.7 (6,6a)

Fig. 7 (1, 1a – 6, 6a). Evolution in stork migration 29.08.2003 , time 10.46 - 14.37. (on the left - echo from all the reflectors, on the right слева – bird vector fields).

### Analysis of the experimental data

Techniques used for collecting and processing experimental data are described in (Dinevich et al., 2001). The meanings of the experimental research units (Average flight altitudes, Maximum flight altitudes, Extreme maximum (for entire observation period), Average level of maximum birds' concentration (for entire period) are given in Appendix.

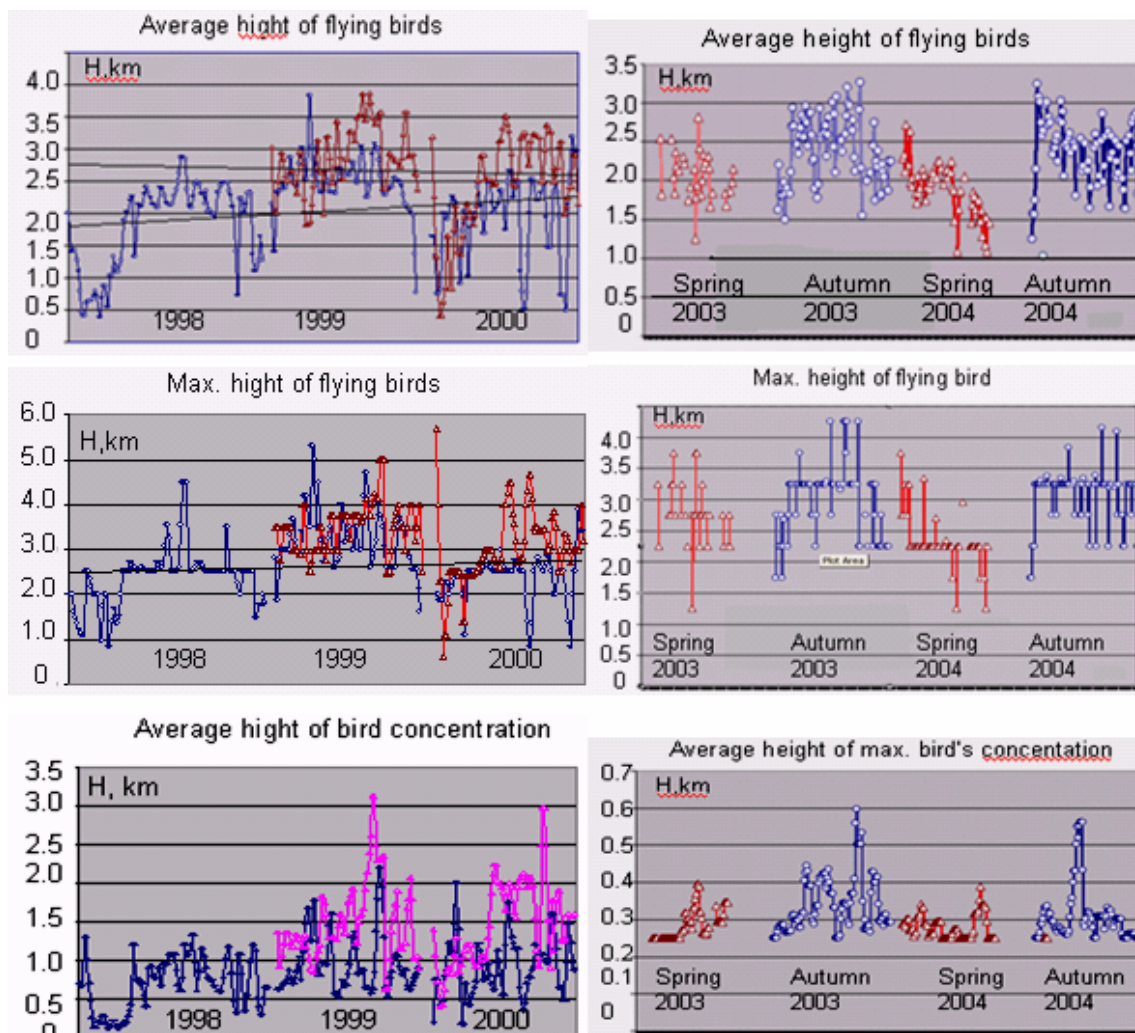


Fig. 8(a, b, c, d, g, h) and Table 4 show the altitude parameters of inter-seasonal bird flights at day time and night time both in spring and in autumn.

**Табл. 4 Altitude parameters of bird migration over Central Israel**

Flight altitudes, m		Spring	Autumn
Average flight altitudes, m	daytime	1,000 - 2,700	1,200 - 3,500
	night	1,900 - 2,600	1,500 - 3,000
Maximum flight altitudes, m	daytime	1,500 - 3,500	1,700 - 4,300
	night	2,900 - 3,600	2,200 - 3,300
Extreme maximum (for entire observation period), m	daytime	3,500*	4,300*
	night	5,700*	5,200*

Average level of maximum birds' concentration (for entire period), m	daytime	250 - 400	250 - 400
	night	250 - 1,500	250 - 1,000

Mean altitude values calculated by the experimental data for nighttime were found to be within the range of 1.900 m - 2.600m in autumn (September-November) and of 1.500m -3.000m in spring. These values are much lower in August (600 m - 1.700m).

In the daytime, mean altitude values were found to be within the range of 1.000 m - 2.700 m in autumn (September-November) and 1.200 m - 3.500 m in spring. The figures clearly show in autumn daytime flights are higher than in spring, while in spring it is vice versa.

**Bird flight velocities and their relationship with the corresponding wind parameters.**

Table 5 presents bird flight velocities in spring and autumn, both in daytime and nighttime.

**Table 5. Bird flight velocities in autumn and in spring**

Velocities, m/sec		Spring	Autumn
Mean velocity	daytime	14	15
	night	14	13
Maximum velocity	daytime	18	16
	night	16	16
Mean wind speed at the ground surface	11h	5.5	5.0
Mean wind speed at the height of 600 m	11h	3 - 6	4 -7

The mean velocity of night flights was found to be:

about 14 m/sec in spring. 24 % of the total number of birds have flight velocities within the range of 10-12 m/c, over 35% within the range of 12-14 m/c and almost 27% within the range of 14-16 m/c; the remaining 14% have a wide range of velocities;

about 13 m/sec in spring. About 7 % of the total number of birds have flight velocities within the range of 10-12 m/c, 70% within the range of 12-16 m/c and almost 11% within the range of 16-18 m/c; the remaining 12% have a wide range of velocities.

The mean velocity of day flights was found to be:

about 14 m/sec in spring. Over 24 % of the total number of birds have flight velocities within the range of 10-12 m/c, over 35% within the range of 12-14 m/c and almost 27% within the range of 14-16 m/c; the remaining 14% have a wide range of velocities;

about 15 m/sec in spring. Over 7 % of the total number of birds have flight velocities within the range of 13-14 m/c, over 70 within the range of >14m/s - <16m/c and almost the remaining 12% have a wide range of velocities;

The mean wind speed at the altitude of 600 m (the values close to that where the maximum migrant bird concentration was found) in within the range 4-7 m/s in autumn and 3 - 6 m/s in spring. As can be seen from the table, both mean and maximum values of bird flights are significantly higher than the wind speed values both at the ground surface and at the altitude of 600 m.

**Bird flight directions and their relationship with the corresponding wind parameters.**

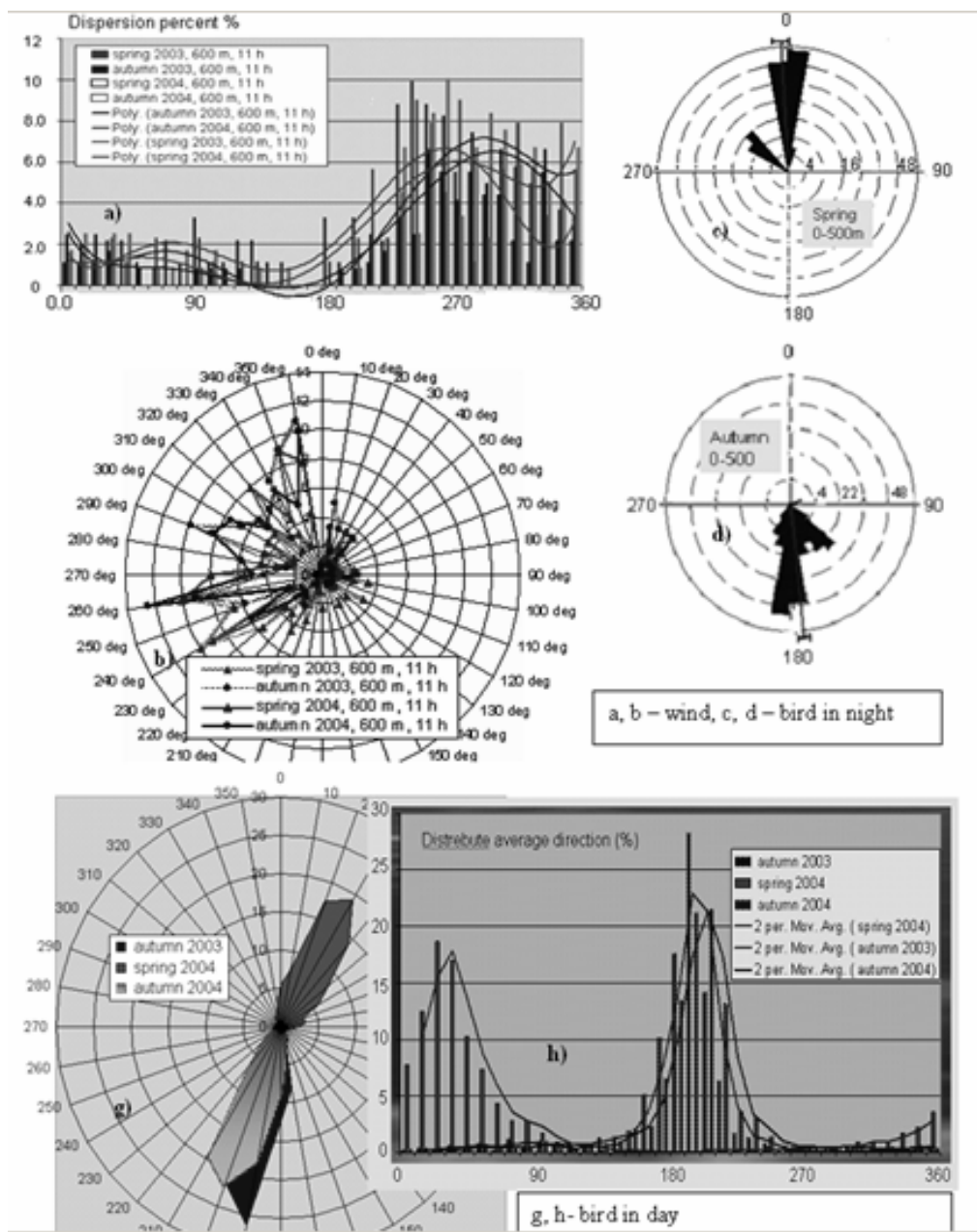
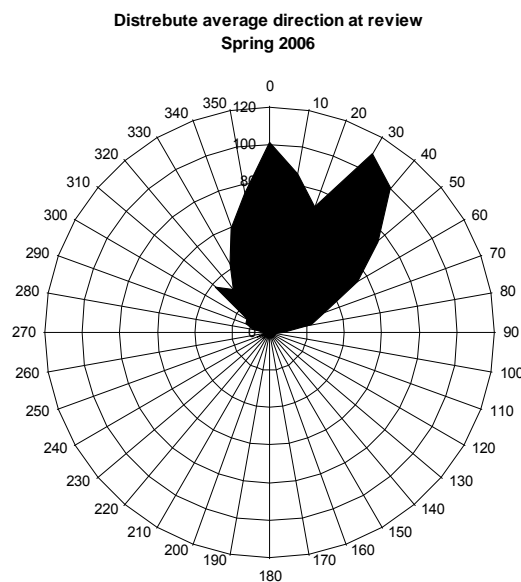


Fig. 9 a) average flight altitudes, b)- maximum flight altitudes, c)- average level of maximum birds concentration (for the entire period) at nighttime. d, g, h : the same for daytime. Autumn data marked blue, spring data marked red.

Fig. 9 (a,b) shows climatological wind rose in autumn and in spring plotted on the basis of Beit Dahan meteorological station (near Tel Aviv) data for the time of 11 a.m. (local time) at the altitude of 600 m over the sea level. This altitude was chosen as it was found to be at the level of maximum day migration. 11 a.m. is the time when maximum day migration is most often observed. Fig.9 (a) presents a recurrence graphs for wind directions (in %) within azimuth sectors in autumn and in spring. As can be seen in the graphs the dominant wind direction both in autumn and in spring is from the sea, the dominant direction in autumn being W-NW and in

spring W- SW (according to the meteorological standards, the wind rose indicated the direction from which wind blows). In contrast, the bird migration graphs show the direction into which birds fly.

Fig. 9 (d,g,k) shows the diagrams of bird flight directions in daytime and nighttime in autumn and in spring.



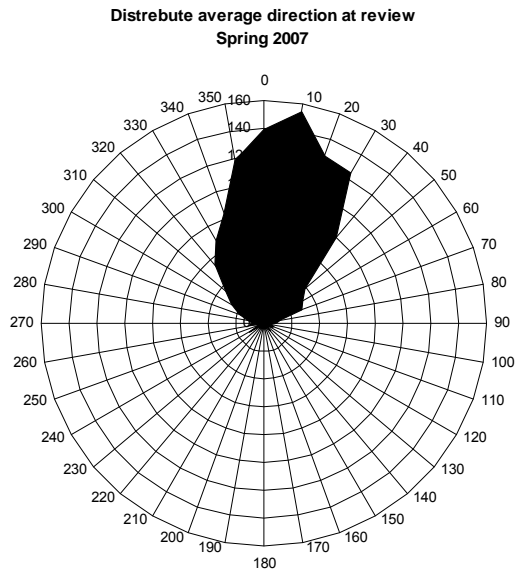


Fig.9 (l,m) shows similar diagrams for daytime in 2006 and 2007. The radius of the wedges corresponds to the observation frequency. The higher probable direction of night migration for 90% birds is  $183^\circ$  in autumn and  $6^\circ$  in spring. We observed bird flocks migration at night time and early morning towards the Mediterranean Sea in spring and from out the Mediterranean Sea in autumn. The sector of these directions is different from the general sector of seasonal migrations being on average  $135^\circ$  in autumn and  $315^\circ$  in spring. This deviation from the dominant direction of migration in the lower altitudes be accounted for by the fact that the birds migrating over the Mediterranean Sea belong to the water-fowl family. Fig. 9 (a, h) shows the spectra of the mean values of seasonal bird migration directions in night and day time, respectively.

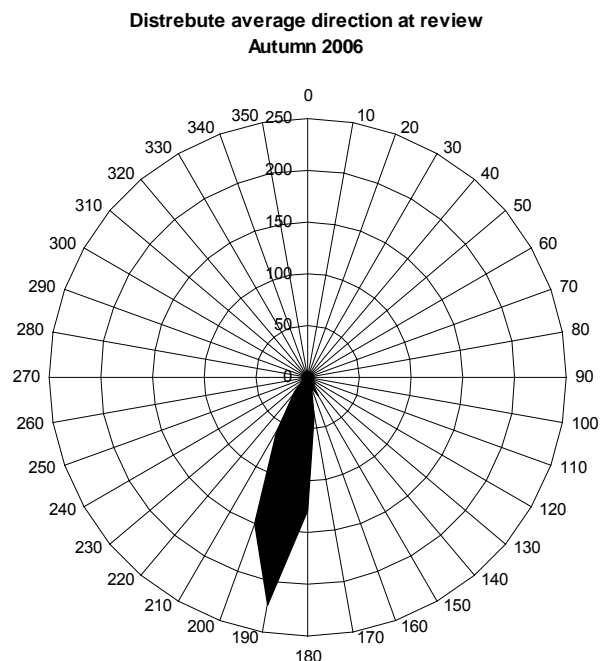


Fig. 9 (m). Distrebut average direction at reviview Autumn

The highest probable direction of daytime migration for 90% birds is  $190^{\circ}$ - $220^{\circ}$  in autumn and  $10^{\circ}$ - $50^{\circ}$  in spring. The spring direction spectrum is much wider than that in autumn.

Comparing figures 9(a-m) one can see that both in autumn and in spring the areas of dominant migration directions coincide with the areas of the most infrequent wind directions. Winds over central Israel most often blow from one side relative to the daytime bird flight migration direction, having no significant impact on the distribution of flight altitudes.

### **Relative changes in migrating birds density at day/nighttime in autumn and spring.**

The accuracy of radar estimation of bird quantities depends on several parameters of the radar ornithological system, among them the surveillance span, receiver sensitivity and errors in the bird identification algorithm. In addition, within the radius of radar surveillance a part of low-flying birds screened by high hills or even fly at the level that is below the radar beam zero level. For example, a part of the bird migration flow over Israel routes along the Jordan Valley and the Dead Sea. The Dead Sea is located at 500 m below the sea level. Since the radar is located at 270 m above the sea level, bird flying altitude of 500m are significantly lower than the beam zero level, and these birds can not be seen by the radar. Taking this into consideration, in order to determine the error in radar estimation of the absolute number of birds currently in the air, further research and special techniques are required.

Nevertheless, using the same technique for collecting data corpus over several years enables to estimate relative bird density within a unit of air volume in autumn and spring, at day and night time.

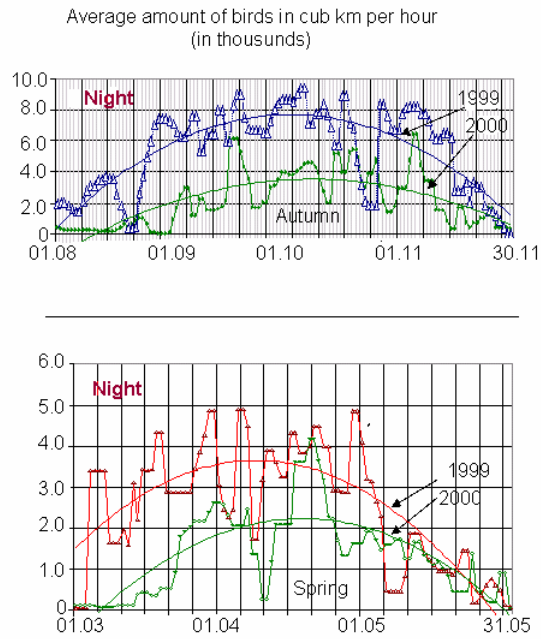


Fig. 10. (a,b): Graph and wind rose of wind directions in autumn (blue color) and spring (red color); c,d: diagrams of bird migration directions at daytime in spring and autumn, respectively; g, h: diagrams and graphs of bird migration at daytime in autumn (blue color) and spring (red color); the same for years 2006 and 2007.

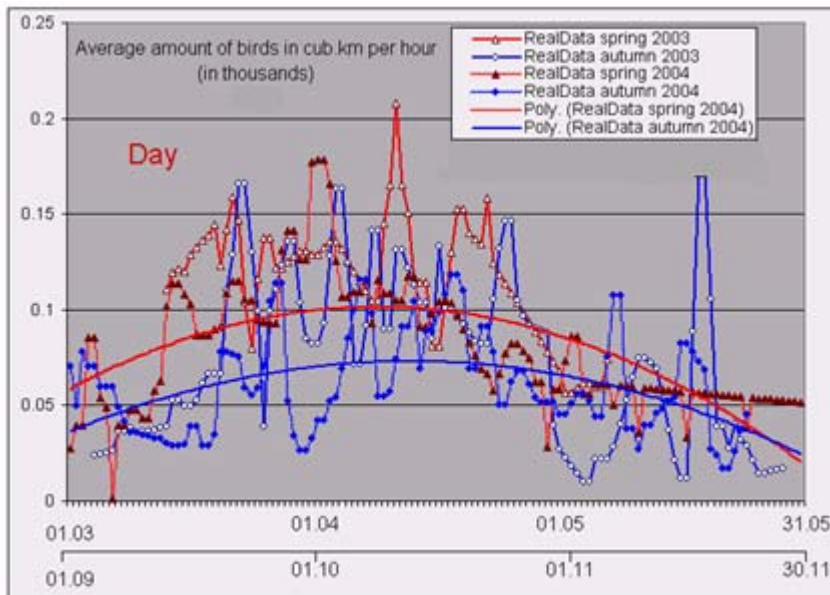


Fig. 10(c). Relative changes in bird quantities within a cubic kilometer of air at day/nighttime in spring and autumn.

These estimations are shown in Fig 10 (a,b,c). According to the data, both at day and night maximum bird quantities cross Central Israel in September-October and in late March-April. At night the number of flying birds is by factor of tens greater than at day time. For example, within a cubic kilometer of air the maximum number of migrating birds can reach 170 ( up to 200 in some cases), while at night this figures approaches 5 thousand in spring and 10 thousand in autumn. The number of birds migrating in autumn significantly exceeds that in spring.

### **General Conclusions.**

-Radar ornithological charts plotted on the basis of the algorithms developed in the study contain the following information collected within the radius of 60 km from the radar

1. the general number of birds currently in the air, among them the number of migrating birds,
2. maximum and minimum bird flight altitudes and velocities,
3. quantitative distribution of bird over altitudes,
4. spectra of flight directions and velocities, including the vector of total direction,
5. vector fields of birds' movement against the background of current meteorological situation and binding to the terrain,
6. distribution of birds by their flight patterns ( degrees of straightforwardness and uniformity).

- The method proposed for bird identification can be applied to using other types of high-grade radars, both coherent and non-coherent ones whose antennas form sharply targeted symmetric beams.

-The research enabled to evaluate the main parameters of bird migration over Central Israel based on a vast corpus of experimental data. These parameters can be used for plotting optimum routes for aircraft.

-The radar ornithological system developed in the study has been efficiently use din Israel for air traffic control.

### **Acknowledgements**

The authors express their gratitude to the Department of Research of the Ministry of Defense of Israel and The Israeli Ministry of Immigrant Absorption for the financial support of the project; to Ilan Setor, Director of the Israeli Meteorological Agency, for the courtesy of providing the research with meteorological data; to Dmitry Shtivelman for the technical support in the radar maintenance.

## References

- Abshayev M., Burtsev I., Vaksenburg S., Shevela G., 1980. Guide for use of the MRL-4, MRL5 and MRL-6 radars in urban protection systems. L., "Hydrometeoizdat".
- Abshayev M., Kaplan L., Kapitannikov A., 1984. Form reflection of meteorologic targets at the primary processing of the meteorologic radar signal. Transactions of VGI, Bd 55.
- Alpert, P., D. S. Tannhauser, (2000). "Migrating soaring birds align along sea-breeze fronts; First evidence from Israel." Bulletin of the American Meteorological Society 81(7): 1599-1601.
- Atlas D., 1964. Advances in Radar Meteorology. – Adv. in Geophys. Vol. 10, p. 318-468.
- Bahat O. and Oded Ovadia, 2005. Minimizing Bird-Aircraft Collisions Caused by Resident Raptors in Israel. IBSC 27<sup>th</sup> Meeting, Athens, Hellas, 23-27 May, p. 178.
- Bruderer B. and Joss, 1969. Zur Registrierung and Interpretation von Echosingnaturen an enema 35 cm-Zielverfolgungstradar. Orn. Beob., Bd 66, 70-88.
- Bruderer B. 1992. Radar studies on Bird migration in the south of Israel. BSCE/21, Jerusalem, pp. 269-280.
- Buurma, L., 1999. The Royal Netherlands Air Force: Two Decades Of Bird Strike Prevention "En Route". International Seminar on Birds and Flight Safety in the Middle East, Israel, April, 25 - 26, 1999. Pp. 71-83.
- Chernikov A., 1979. Radar clear sky echoes. Leningrad, Hydrometeoizdat, 3-40.
- Chernikov A., Schupjatsky A., 1967. Polarization characteristics of radar clear sky echoes. Transactions of USSR academy of sciences, atmosphere and ocean physics, V.3, N2, 136-143.
- Dinevich L., Kapitalchuk I., Schupjatsky A., 1990. Measurement of the microphysical characteristics of clouds and precipitation with a dual-polarization radar. In: Artificial modification of atmospheric processes in Moldova, iss2., Kiscinev.
- Dinevich L., Kapitalchuk I., Schupjatsky A., 1994. Use of the polarization selection of radar signals for remote sounding of clouds and precipitation. 34 th Israel Annual conference on Aerospace science, 273-277.
- Dinevich L., Leshem I., Gal A., Garanin V., Kapitannikov A., 2000. Study of birds migration by means of the MRL-5 radar. J. Scientific Israel –Technological Advantages. Vol. 4.
- Dinevich L., Kaplan L. 2000. On Radar observation of Birds migration. J. Scientific Israel –Technological Advantages. Vol. 4.
- Dinevich L., Leshem Y., Sikora, O., 2001. RADAR OBSERVATIONS ANALYSIS OF SEASON BIRD MIGRATION IN ISRAEL AT NIGHT (Based on data of radar photo registration obtained in 1998-2000), J. Scientific Israel –Technological Advantages, Vol. 3, 2001, No. 1-2.
- Dinevich L., Leshem Y., Pinsky M., Sterkin A., 2004. Detecting Birds and Estimating their Velocity Vectors by Means of MRL-5 Meteorological Radar. J. The Ring 26, (2): 35-53.
- Dinevich L., Leshem Y., 2008. Algorithmic system for identifying bird radio-echo and plotting radar ornithological charts. J. The Ring 28, 2: 3-39.
- Eastwood E., 1967. Radar ornithology. London, Methuen, 278.
- Edwards J., Houghton E. W., 1959. Radar echoing area polar. Diagrams of birds.-Nature, 184, N. 4692.
- Houghton E, 1964. Detection, recognition and identification of birds on radar. In: World conf. Radio Met., Amer. Met. Soc., Boston, 14-21.
- Doviak, R., Zrnic, D., 1984. Doppler Radar and Weather Observation. Akademic Press Inc., 512pp.
- Gauthreaux, S. A. and C. G. Belser (2003). "Radar ornithology and biological conservation." Auk 120(2): 266-277.

- Ganja I., Zubkov M., Kotjazi M., 1991. Radar ornithology, *Stianza*, 123-145.
- Gudmundsson, G. A., T. Alerstam, et al. (2002). "Radar observations of Arctic bird migration at the Northwest Passage, Canada." *Arctic* 55(1): 21-43.
- Gauthreaux, Sidney A. Jr., David S. Mizrahi, and Carroll G. Belser. 1998. Bird Migration and Bias of WSR-88D Wind Estimates. *Weather and Forecasting* 13:465-481.
- Glover K., Hardy K., 1966. Dot angels: insects and birds.-In: Proc. 12<sup>th</sup> Weather Radar Conf., Amer. Met. Soc., Boston, p. 264-268.
- Houghton E, 1964. Detection, recognition and identification of birds on radar. In: World conf. Radio Met., Amer. Met. Soc., Boston, 14-21.
- Hajovsky R., Deam A., La Grone A., 1966. Radar reflections from insects in the lower atmosphere.-IEEE Trans. On Antennas and Propagation, vol.14, pp224-227.
- Khardy K., 1969. Зондирование безоблачной атмосферы с помощью мощных радиолокаторов с высоким разрешением.—«Труды института инженеров по электротехнике и радиоэлектронике». Т. 57, № 4. Пер. с англ. М., «Мир», с. 109—112.
- Komenda-Zehnder, S., F. Liechti, et al. (2002). "Is reverse migration a common feature of nocturnal bird migration. An analysis of radar data from Israel." *Ardea* 90(2): 325-334.
- Kropfli R. A., 1970. Simultaneous radar and instrumented aircraft observations in a clear air turbulent layer.- In: Prepr. 14<sup>th</sup> Radar Met. Conf., Amer. Met. Soc., Boston, p. 117-120.
- Larkin, R. P., W. R. Evans, et al. (2002). "Nocturnal flight calls of Dickcissels and Doppler radar echoes over south Texas in spring." *Journal of Field Ornithology* 73(1): 2-8.
- Leshem, Y., Y. Yom-Tov. 1998. Routes of migrating soaring birds. *Ibis* 140, 41-52.
- Leshem, Y. and S. A. Gauthreaux, 1996. Proposal to develop a global network to predict bird movements on a real-time and daily scale by using radars. Bird Strike Committee Europe BSCE-23/WP 50. London, May 13-17.
- Leshem, Y., Y. Yom-Tov 1996. The use of thermals by soaring migrants in Israel. *Ibis* 138, 667-674.
- Lofgren G., Battan L., 1969. Polarization and vertical velocities of dot angel echoes. – *J. Appl. Met.*, pp. 948-951.
- Miller, M. A., J. Verlinde, et al. (1998). "Detection of nonprecipitating clouds with the WSR-88D: a theoretical and experimental survey of capabilities and limitations." *Weather and Forecasting* 13(4): 1046-1062.
- Oded Ovadia, Maj., M. Sc., Israel and Nicholas B. Carter, Ph.D., USA. 2005. A Paradigm Shift in Bird Strike Prevention by the Israeli Air Force. IBSC. 27<sup>th</sup> Meeting. Athens, Hellas, 23-27 May 2005. pp. 57-58.
- Venema, V., H. Russchenberg, et al. (2000). "Clear-air scattering observations: downdraft and angels." *Physics and Chemistry of the Earth. B: Hydrology* 25(10-12): 1123-1128.
- Richardson W. J. and T. West, 2005. Serious Birdstrike Accidents to U. K. Military Aircraft, 1923 to 2004: Numbers and Circumstances. IBSC 27<sup>th</sup> Meeting, Athens, Hellas, 23-27 May, p. 5.
- Russell, K. R. and S. A. Gauthreaux (1998). "Use of weather radar to characterize movements of roosting purple martins." *Wildlife Society Bulletin* 26(1): 5-16.
- Сальман Е., Брылёв Г., 1961. Радиоэхо диэлектрических неоднородностей термического характера. Тр. ГГО, вып. 120, с.37-44.
- Skolnik, M., 1970. RADAR HANDBOOK. MCGRAW-HILL BOOK COMPANY.
- Schaefer G., 1966. The study of birds echoe using a tracking radar. Proc. 14<sup>th</sup> Int. Ornith. Cjngress. Oxford.
- Schaefer G., 1968. Bird recognition by radar: a study in quantitative radar ornithology. The problems of birds ad pests. London; New York.

- Шестаков Г., 1971. Строение крыльи и механика полёта птиц. Москва, 180с.
- Shupijatsky A., 1959. Радиолокационное рассеяние несферическими частицами, Тр. ЦАО, вып. 30, с. 39-52.
- Stepanenko V., 1973. Радиолокация в метеорологии. Гидрометеоздат. Ленинград.
- Thorpe J., 2005. Fatalities and Destroyed Civil Aircraft Due to Bird Strikes, 2002 to 2004 (with an Addendum of Animal Strikes). IBSC 27<sup>th</sup> Meeting, Athens, Hellas, 23-27 May, p. 17-24.
- Zavirucha V., Saricev V., Stepanenko V, Shepkin U., 1977. Study of the dispersion characteristics of the meteorological and ornithological objects in echo-free cameras *Proc. Main Geophysic Observatory*, #395, с. 40 –45.
- Zrnic, D. S. and A. V. Ryzhkov (1998). "Observations of insects and birds with a polarimetric radar." *Ieee Transactions on Geoscience and Remote Sensing* 36(2): 661-668.
- Якоби В. Э. Биологические основы предотвращения столкновений самолётов с птицами. Москва, 1974, 165с.

## Appendix. Glossary and Symbols.

1. Radar reflectance ( $Z$  or  $\eta$ ) characterizes the dispersive properties of a target within the ranges of the waves used. Its value depends on the target's dimensions, concentration of targets within the surveillance area, as well as on the dielectric properties of targets and wavelength (for details see Stepanenko, 1973)
2. Effective scattering area ( $\sigma$ ) characterizes a target's square in  $\text{cm}^2$  or  $\text{m}^2$  but depends on the of targets and wavelength (for details see Skolnik, 1970)
3. Differential reflectance (dP) characterizes the ellipticity of a target and its orientation in the space. For globular targets (e.g. small drops) it approaches zero dB, while for non-globular targets horizontally oriented in the space (e.g. birds) its values is significantly greater than unity (for details see Shupijatsky, 1959; Zrnic and Ryzhkov, 1998 )
4. The polarization device attached to MRL-5 enables to alter the polarization of the radiated signal pulse-by pulse, from the horizontal to the vertical one and vice versa, as well as to measure the polarization parameters of the echo and their correlations.
5. The device for measuring signal fluctuation is a peak detector that enables to isolate and to store in a digital form all the maximum signal values per pulse within any 200m-long strobe selected on the radar
6. during a certain time segment (usually 10-15 sec). On the basis if samples thus obtained the software lots their spectrograms with exact binding to the measurement time and target coordinates. The spectrogram is the function of changeability of the target's reflectance in time.
7. Average flight altitudes , Maximum flight altitudes, Average level of maximum birds' concentration (for entire period) are calculated using formulas

$$\overline{H_{\max}} = \frac{1}{m} \sum_{i=1}^m \frac{1}{k} \sum_{j=1}^k h_{mij} \quad (1); \quad H_{\max} := \max \{ \max [h_{mij}] \} \quad (2); \quad \overline{H_{\max.con}} = \frac{1}{m} \sum_{i=1}^m \frac{1}{k} \sum_{j=1}^k h_{m.con.ij} \quad (3)$$

where  $\overline{H_{\max}}$  is the mean maximum bird flight altitude over a prescribed period (observation series during a single day or night);

$\overline{H_{\max.con}}$  is the analogous mean maximum bird density value;

$H_{\max}$  is the maximum over all maximum bird flight altitudes over a prescribed period;  
 $j =$  from 1 to  $m$  is the number of night (daytime) observations,  $i =$  from 1 to  $k$  is the number an-hour long observations conducted during a given night (day);  
 $h_{mij}; h_{mcon.ij}$  is, respectively, the maximum altitude and the maximum bird density over each single observation.